

# Syntheses and Characterizations of two Zinc(II) Metal-organic Frameworks based on 1,4-Naphthalenedicarboxylate and Imidazole Ligands

Jingyuan Wang\*<sup>[a]</sup> and Hongpeng You\*<sup>[a]</sup>

**Keywords:** Metal-organic frameworks; 2-Phenylimidazole; 1,1'-(1,4-Butanediyl)bis(imidazole); 1,4-Naphthalenedicarboxylate; Luminescence; Zinc

**Abstract.** Two new compounds, namely  $[\text{Zn}(1,4\text{-ndc})(\text{L}1)]$  (**1**), and  $[\text{Zn}(1,4\text{-ndc})(\text{L}2)]\cdot 0.25\text{H}_2\text{O}$  (**2**) [ $\text{L}1 = 2\text{-phenylimidazole}$ ,  $\text{L}2 = 1,1'\text{-}(1,4\text{-butanediyl})\text{bis}(\text{imidazole})$ , and  $1,4\text{-ndc} = 1,4\text{-naphthalenedicarboxylate}$ ] were successfully synthesized under similar hydrothermal conditions. In compound **1**, each 1,4-ndc anion links two neighboring  $\text{Zn}^{\text{II}}$  cations with its carboxylate groups to generate a 2D layer structure. The L1 ligands are attached on both sides of the layers. In com-

pound **2**, each carboxylate group of 1,4-ndc connects one  $\text{Zn}^{\text{II}}$  atom in monodentate mode to form a 1D zigzag chain. Further, the L2 ligands link the chains to generate an expanded diamond net. Four diamond networks interweave to form a 3D interpenetrating diamond framework in an unusual [2+2] mode. Furthermore, the title compounds exhibit good luminescent properties in the range from ultraviolet to visible light and may find potential applications as fluorescent materials.

## 1. Introduction

The rational design and synthesis of metal-organic frameworks (MOFs) have attracted considerable attention due to their interesting topologies and potential applications in non-linear optics, magnetism, molecular recognition, gas adsorption, etc.<sup>[1]</sup> With the development of supramolecular chemistry and crystal engineering of MOFs, it is possible to design and construct novel MOFs with desired topologies and rationally predict the final structures of the product.<sup>[2]</sup> Generally, the diversity in the framework structures greatly depends on the selection of the metal, the inorganic counterion, the solvent system, and sometimes the metal-to-ligand ratio.<sup>[3]</sup> In this regard, the selection of the ligand is an important factor that may be utilized in determining the framework topology, which has not been widely employed to date.<sup>[4]</sup> The changes in functional group, flexibility, length, and symmetry of the ligands can result in a remarkable class of materials with diverse architectures and functions. Among them, the rigid organic polycarboxylates are often employed as bridging ligands to afford a variety of novel functional complexes due to their versatile coordination modes.<sup>[5]</sup> On the other hand, nitrogen-donor ligands have been intensely investigated for the construction of novel MOFs, and the use of nitrogen-donor ligands is an effective method because they can satisfy and even mediate the coordination needs of the metal atoms and consequently generate more meaningful architectures.<sup>[6]</sup> So far, the rigid nitrogen-donor ligands (4,4'-bipyridine, pyrazine, etc.) have been exten-

sively employed in the construction of a rich variety of intriguing architectures. However, the imidazole-containing ligands have not been well studied.<sup>[7]</sup>

Recent studies have demonstrated that mixed organic ligands, especially the mixed polycarboxylate and nitrogen-containing ones with more tunable factors, are good candidates for the construction of novel MOFs. Following such a mixed-ligand strategy, we focused our attention in this study on the reactions of the ligand 1,4-naphthalenedicarboxylate (1,4-ndc) with different imidazole ligands and  $\text{Zn}^{\text{II}}$  salts and made a systematic investigation on the impact of imidazole ligands on the structures of the complexes. Herein, we report the syntheses, crystal structures, and photoluminescent properties of two new  $\text{Zn}^{\text{II}}$  MOFs with two different imidazole ligands, namely,  $[\text{Zn}(1,4\text{-ndc})(\text{L}1)]$  (**1**), and  $[\text{Zn}(1,4\text{-ndc})(\text{L}2)]\cdot 0.25\text{H}_2\text{O}$  (**2**) [ $\text{L}1 = 2\text{-phenylimidazole}$  and  $\text{L}2 = 1,1'\text{-}(1,4\text{-butanediyl})\text{bis}(\text{imidazole})$ ]. Complexes **1** and **2** were characterized by IR spectroscopy and X-ray crystallography.

## 2. Experimental Section

All reagents and solvents for syntheses were purchased from commercial sources and used as received. Powder X-ray diffraction (XRD) data were collected with a Siemens D5005 diffractometer with  $\text{Cu-K}\alpha$  radiation ( $\lambda = 1.5418 \text{ \AA}$ ). Inductively coupled plasma (ICP) analysis was performed with a Perkin-Elmer Optima 3300DV spectrometer. Elemental analysis was conducted with a Perkin-Elmer 2400 elemental analyzer. Thermogravimetric analyses (TGA) were carried out with a NETZSCH STA 449C TGA/DTA analyzer in air with a heating rate of  $10 \text{ }^\circ\text{C}\cdot\text{min}^{-1}$ . IR spectra were recorded with a Bruker TENSOR 27 Fourier Transform Infrared Spectrometer using KBr pellet. Fluorescent emission spectra for the solid samples were recorded with a Hitachi F-4500 luminescence spectrometer.

\* Dr. J. Wang  
E-Mail: wangjingyuan1208@gmail.com

\* Prof. Dr. H. You  
E-Mail: hpyou@ciac.jl.cn

[a] State Key Laboratory of Rare Earth Resource Utilization  
Changchun Institute of Applied Chemistry  
Changchun 130022, P. R. China

## 2.1. Syntheses of the Metal Complexes

### 2.1.1. Synthesis of [Zn(1,4-ndc)(L1)] (1)

A mixture of 1,4-ndc (0.216 g, 1 mmol), L1 (0.15 g, 1 mmol), ZnCl<sub>2</sub> (0.136 g, 1 mmol), NaOH (0.08 g, 2.00 mmol), and H<sub>2</sub>O (12 mL) was stirred for 1 h and afterwards sealed in a 25 mL Teflon-lined stainless steel container. The container was heated at 140 °C for 3 days. After slow cooling, colorless block crystals of **1** were yielded along with some unidentified yellow powder. The crystalline samples of **1** were picked for the analysis in ca. 52 % yield. The product was initially characterized by elemental analyses and ICP and the data were as follows: found C 59.21; H 3.67; N 6.45; Zn 15.59 %; anal. calcd: C 59.52; H 3.33; N 6.61; O 15.10; Zn 15.43 %. IR (KBr):  $\tilde{\nu}$  = 3744 (w), 3112 (w), 2853(w), 1610 (m), 1562 (s), 1350 (m), 1224 (m), 1121 (m), 833 (m), 783 (w) cm<sup>-1</sup>.

### 2.1.2 Synthesis of [Zn(1,4-ndc)(L2)]·0.25H<sub>2</sub>O (2)

Complex **2** was obtained by a similar procedure to that used for preparation of **1** except for using L2 (0.185 g, 1 mmol) instead of L1 as starting material. Colorless block crystals of **2** were manually isolated and washed with water several times in 39 % yield. Elemental analyses and ICP data were as follows: found: C 55.21; H 4.54; N 11.60; Zn 13.97 %; anal. calcd: C 55.71; H 4.36; N 11.82; O 14.34; Zn 13.78 %. IR (KBr):  $\tilde{\nu}$  = 3742 (w), 3103 (w), 2930 (w), 1650 (s), 1614 (m), 1363 (m), 1318 (m), 1223 (m), 822 (w), 791 (m) cm<sup>-1</sup>.

## 2.2. X-ray Crystallography

Single-crystal X-ray diffraction data for compounds **1** and **2** were recorded with a Bruker Apex CCD diffractometer with graphite-monochromated Mo-K<sub>α</sub> radiation ( $\lambda$  = 0.71073 Å) at 293 K. Absorption corrections were applied using multi-scan technique. All the structures were solved by Direct Methods with SHELXS-97<sup>[8]</sup> and refined by full-matrix least-squares techniques using SHELXL-97<sup>[9]</sup> within WINGX. Non-hydrogen atoms were refined with anisotropic temperature parameters. The disordered carboxylate oxygen atoms (O4 and O4') in compound **2** were refined using oxygen atoms split over two sites, with a total occupancy of 1. The hydrogen atoms attached to carbons were generated geometrically; the aqua hydrogen atoms of **2** were not located from difference Fourier maps.

Detailed crystallographic data and structure refinement parameters for **1** and **2** are summarized in Table 1, and selected bond length and bond angle data are summarized in Table 2.

**Table 1.** Crystal data and structure refinements for compounds **1** and **2**.

	<b>1</b>	<b>2</b>
Formula	C <sub>21</sub> H <sub>14</sub> N <sub>2</sub> O <sub>4</sub> Zn	C <sub>22</sub> H <sub>20.5</sub> N <sub>4</sub> O <sub>4.25</sub> Zn
Molecular weight	423.71	474.29
Crystal system	Orthorhombic	Monoclinic
Space group	<i>Pbca</i>	<i>C2/c</i>
<i>a</i> / Å	16.6595(6)	17.779(4)
<i>b</i> / Å	12.7896(5)	18.305(4)
<i>c</i> / Å	17.4093(6)	15.540(4)
$\beta$ / °		123.389(4)
<i>V</i> / Å <sup>3</sup>	3709.4(2)	4222.9(18)
<i>Z</i>	8	8
GOF	1.055	1.042
<i>R</i> <sub>1</sub> [ <i>I</i> > 2σ( <i>I</i> )] <sup>a</sup>	0.0385	0.0549
<i>wR</i> <sub>2</sub> (all data) <sup>b</sup>	0.0615	0.1598

a)  $R_1 = \sum ||F_o| - |F_c|| / \sum |F_o|$ . b)  $wR_2 = [\sum w(|F_o|^2 - |F_c|^2) / \sum w(F_o^2)]^{1/2}$ .

CCDC-785008 and CCDC-785009 contain the supplementary crystallographic data for **1** and **2**. These data can be obtained free of charge via <http://www.ccdc.cam.ac.uk/conts/retrieving.html>, or from the Cambridge Crystallographic Data Centre CCDC, 12 Union Road, Cambridge CB2 1EZ, UK; Fax: +44-1223-336-033; or E-Mail: [deposit@ccdc.cam.ac.uk](mailto:deposit@ccdc.cam.ac.uk).

## 3. Results and Discussion

### 3.1 Descriptions of Crystal Structures

#### 3.1.1 Structure of [Zn(1,4-ndc)(L1)] (1)

X-ray single crystal diffraction revealed that complex **1** has a 2D layer structure. The asymmetric unit consists of one zinc(II) ion, one 1,4-ndc ligand, and one unique L1 ligand. As shown in Figure 1, the Zn<sup>II</sup> atom shows a distorted {ZnNO<sub>4</sub>} square pyramidal arrangement, which is coordinated by one nitrogen atom (N1) from one L1 ligand, and four carboxylate oxygen atoms (O2A, O3A, and O4A) from three different 1,4-ndc anions. The Zn–O and Zn–N distances range from 1.974 to 2.015 Å, which are similar to the reported values. Both carboxylate groups of 1,4-ndc ligand are deprotonated during the reaction and the ligand adopts a bidentate bridging mode to link two zinc ions. In this mode, each 1,4-ndc anion links two neighboring Zn<sup>II</sup> cations with carboxylate groups to generate a 2D layer structure (Figure 2). The L1 ligands are attached on both sides of the layers. From the topological view, if the dinuclear Zn<sup>II</sup> ions are considered as four-connected nodes, compound **1** shows a 2D (4,4) topological network. Further, the resulting (4,4) networks are packed in a parallel fashion (Figure 3). The adjacent layers are further connected through intermolecular N–H⋯O hydrogen bonds (N2–H2⋯O4 2.764(4) Å) to extend the 2D layers in to a 3D supramolecular framework.

#### 3.1.2 Structure of [Zn(1,4-ndc)(L2)]·0.25H<sub>2</sub>O (2)

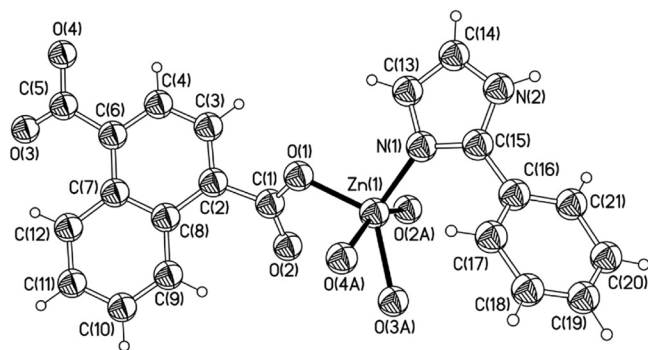
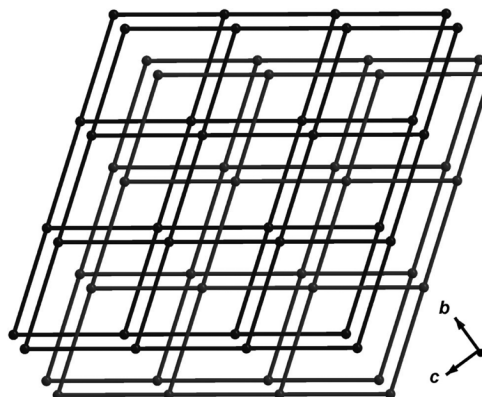
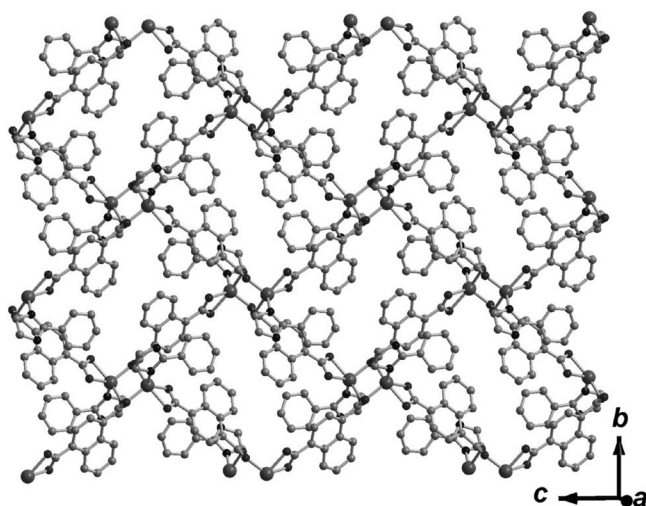
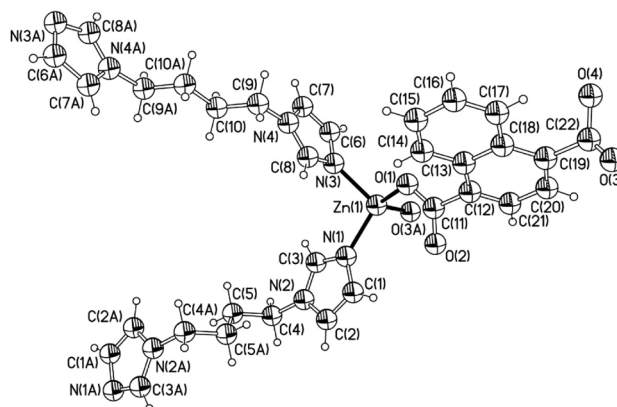
To study the influence of the arrangement and flexibility of imidazole ligands in the formation of the final structures, the ligand L2 was selected to react with 1,4-ndc under similar synthetic conditions, and a structurally different complex [Zn(1,4-ndc)(L2)]·0.25H<sub>2</sub>O (**2**) was obtained. X-ray single crystal diffraction revealed that complex **2** shows an unusual 3D fourfold interpenetrating diamond structure. The asymmetric unit consists of one zinc ion, one 1,4-ndc ligand and two half L2 ligands. As illustrated in Figure 4, each central Zn<sup>II</sup> atom is coordinated by two oxygen atoms (Zn–O 2.199(3)–2.211(3) Å) of two different 1,4-ndc anions and two nitrogen atoms (Zn–N 2.198(4)–2.231(4) Å) of two different L2 ligands to furnish a disordered tetrahedral arrangement.

Notably, the coordination mode of 1,4-ndc in **2** is entirely different from that in **1**. Each carboxylate group connects one Zn<sup>II</sup> atom in monodentate mode to form a 1D zigzag chain. Further, the L2 ligands link the chains to generate an expanded diamond net. Figure 5a,b shows a single cage delimited by four cyclohexane-like windows in chair conformations. Water molecules are found in the adamantane cages of the network. As shown in Figure 6, the hexagonal channels of

**Table 2.** Selected bond lengths /Å and bond angles /° for compounds **1** and **2**.

1		2	
O(1)–Zn(1)	1.991(2)	N(1)–Zn(1)	2.002(4)
O(2)–Zn(1)#2	2.032(2)	N(3)–Zn(1)	2.011(4)
O(3)–Zn(1)#1	2.093(2)	O(1)–Zn(1)	1.981(4)
O(4)–Zn(1)#1	2.196(2)	O(3)–Zn(1)#3	1.917(5)
Zn(1)–N(1)	1.998(2)	Zn(1)–O(3)#4	1.917(5)
Zn(1)–O(2)#2	2.032(2)	O(3)#4–Zn(1)–O(1)	110.7(3)
Zn(1)–O(3)#3	2.093(2)	O(3)#4–Zn(1)–N(1)	103.3(3)
Zn(1)–O(4)#3	2.196(2)	O(1)–Zn(1)–N(1)	122.2(2)
O(1)–Zn(1)–N(1)	101.44(11)	O(3)#4–Zn(1)–N(3)	122.4(2)
O(1)–Zn(1)–O(2)#2	102.85(9)	O(1)–Zn(1)–N(3)	96.23(19)
N(1)–Zn(1)–O(2)#2	95.58(10)	N(1)–Zn(1)–N(3)	103.35(17)
O(1)–Zn(1)–O(3)#3	128.63(9)		
N(1)–Zn(1)–O(3)#3	124.32(11)		
O(2)#2–Zn(1)–O(3)#3	95.25(9)		
O(1)–Zn(1)–O(4)#3	90.62(9)		
N(1)–Zn(1)–O(4)#3	101.95(10)		
O(2)#2–Zn(1)–O(4)#3	155.34(8)		
O(3)#3–Zn(1)–O(4)#3	60.51(8)		

Symmetry transformations used to generate equivalent atoms for **1**: #1  $x, -y-1/2, z-1/2$ ; #2  $-x+1, -y, -z$ ; #3  $x, -y-1/2, z+1/2$ . Symmetry transformations used to generate equivalent atoms for **2**: #1  $-x+1/2, -y-1/2, -z$ ; #2  $-x+1/2, -y-1/2, -z+1$ ; #3  $x+1/2, -y+1/2, z+1/2$ ; #4  $x-1/2, -y+1/2, z-1/2$ .

**Figure 1.** Coordination environment of the Zn<sup>II</sup> ion in compound **1**.**Figure 3.** The stacking mode of two layers of **1**.**Figure 2.** View of a single layer of **1**.**Figure 4.** Coordination environment of the Zn<sup>II</sup> ion in compound **2**.

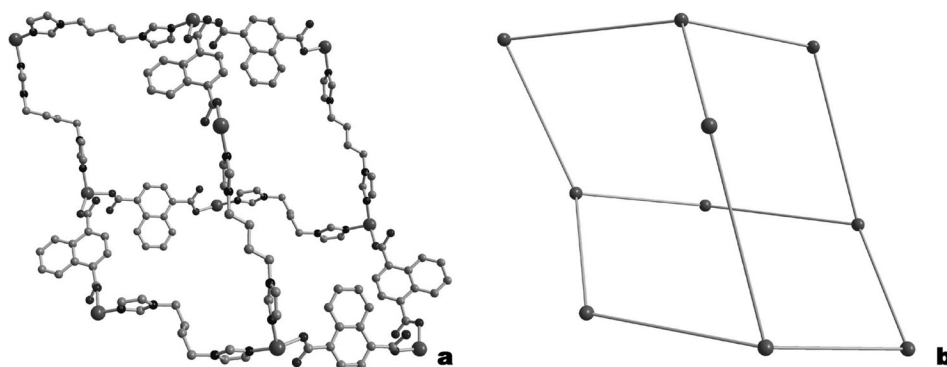


**Figure 5.** (a) Single adamantanoid cage in compound **2**. (b) Schematic representation of single adamantanoid cage in compound **2**.

25.9 Å × 20.6 Å are expanded from the diamond net (corresponding to the longest intracage Zn···Zn distances) (Figure 6). Because of the large windows in the diamond network the interweaving results are not surprising. Four diamond networks interweave to form a 3D interpenetrating diamond framework in an unusual [2+2] mode, as shown in Figure 7a,b. This interpenetration mode differs from the normal mode and can be described as two sets of normal 2- and twofold nets, that is, an unusual [2+2] mode of interpenetration.

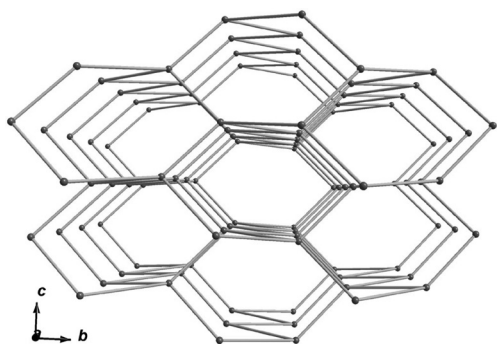


**Figure 6.** Schematic representation of the diamond net of **2**.

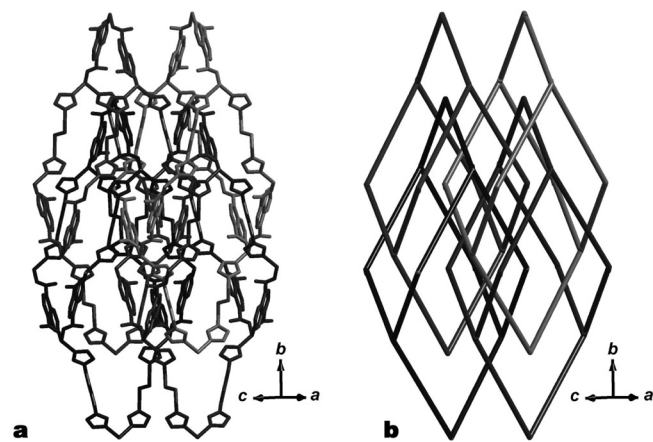


**Figure 7.** (a) Four interpenetrating diamondoid cages in compound **2**. (b) Schematic representation of the four interpenetrating diamondoid cages in compound **2**.

It should be noted that the N-donor ligand plays an important function in the formation of the final structure. In compounds **1** and **2**, the structural differences are primarily affected by the introduction of the N-donor ligands. L1 is a rigid monodentate imidazole ligand with a phenyl group, whereas L2 is a flexible bidentate imidazole ligand. The additional imidazole groups in the backbone may significantly increase the dimensions of their structures, leading to structural differences in their complexes. In compound **1**, the L1 ligands are attached on both sides of the layers formed by the 1,4-ndc anions and Zn<sup>II</sup> cations. Nevertheless, when a flexible L2 ligand was used under the same reaction condition, the structurally different compound **2** was obtained. In **2**, the L2 ligands link the 1D zigzag Zn-1,4-ndc chains to form a 3D diamond-like structure.

### 3.2. PXRD Patterns of Compounds **1** and **2**

The simulated and experimental PXRD patterns of compounds **1** and **2** are shown in Figure 8. The experimental PXRD patterns are in good agreement with the simulated ones except for the relative intensity variation because of preferred orientations of the crystals. For compounds **1** and **2**, the final products include crystal samples of **1** and **2** and a small amount of powder impurities, respectively. Attempts to prepare monophase materials failed. However, the yields of compounds **1** and **2** were improved when hydrothermal syntheses were used.

### 3.3. Thermal Stability Analysis

To characterize compounds **1** and **2** in more detail, TGA studies were carried out in nitrogen from 35 to 800 °C (Figure 9). The TG curve of compound **1** exhibits one weight loss stage in the temperature range 290–517 °C. The weight loss of 79.10 % can be assigned to the decomposition of 2-phenylimidazole and 1,4-naphthalenedicarboxylate ligands (weight loss calcd. 80.80 %). The TG curve of compound **2** exhibits two weight loss stages in the temperature range 320–650 °C. The total weight loss of **2** is 81.42 %, it can be assigned to the decomposition of 1,1'-(1,4-butanediyl)bis(imidazole) and 1,4-naphthalenedicarboxylate ligands (weight loss calcd. 81.90 %).

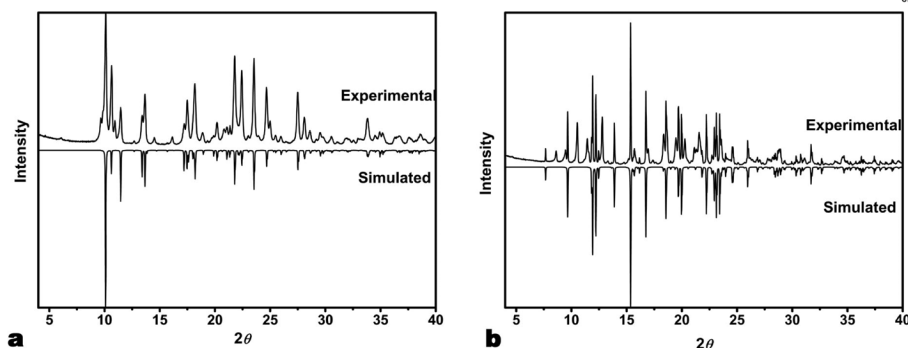


Figure 8. Experimental and simulated XRD patterns for **1** (a) and **2** (b).

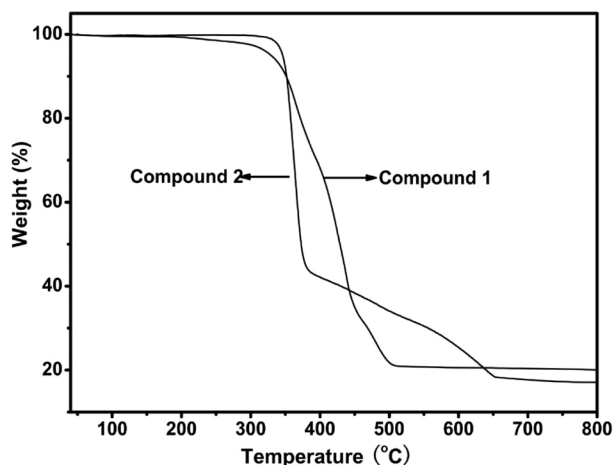


Figure 9. Thermogravimetric analysis curves for compounds **1** and **2**.

### 3.4. Photoluminescent Properties

The photoluminescent properties of compounds **1** and **2** were investigated at room temperature. As shown in Figure 10, the title compounds show interesting photoluminescence. The emission spectrum of compound **1** shows a broad signal at 385 nm when an excited at 353 nm. When excited at 272 nm, compound **2** exhibits a main signal at about 324 nm. The emission bands of compounds **1** and **2** are assigned to ligand-to-metal-charge-transfer (LMCT). Both N-donor and O-donor li-

gands show contribution to the fluorescence of compounds **1** and **2** simultaneously. The difference in their emissions is probably due to the differences in organic ligands and coordination environment around the metal ions, because the photoluminescence behavior is closely associated with the metal ions and the organic ligands coordinated around them. These observations suggest that these compounds could be anticipated as potential fluorescent materials.

## 4. Conclusions

Two new zinc-organic compounds were successfully crystallized through the variation of the N-donor ligands. In compound **1**, 1,4-ndc anions link Zn<sup>II</sup> cations to generate a 2D layer structure. The 2-phenylimidazole ligands are attached on both sides of the layers. In compound **2**, each carboxylate group of 1,4-ndc connects one Zn<sup>II</sup> atom in monodentate mode to form a 1D zigzag chain. Further, the 1,1'-(1,4-butane-diyl)bis(imidazole) ligands link the chains to generate an expanded diamond net. Four diamond networks interweave to form a 3D interpenetrating diamond framework in an unusual [2+2] mode. The results suggest that the structural diversification of MOFs may result from the different coordination modes of organic ligands and the coordination arrangement of metal ions. Our current studies on ligand effect are helpful in achieving further insights into the rational design and construction of diverse MOFs through the intelligent selection of the ligands under corresponding conditions. Moreover, the title com-

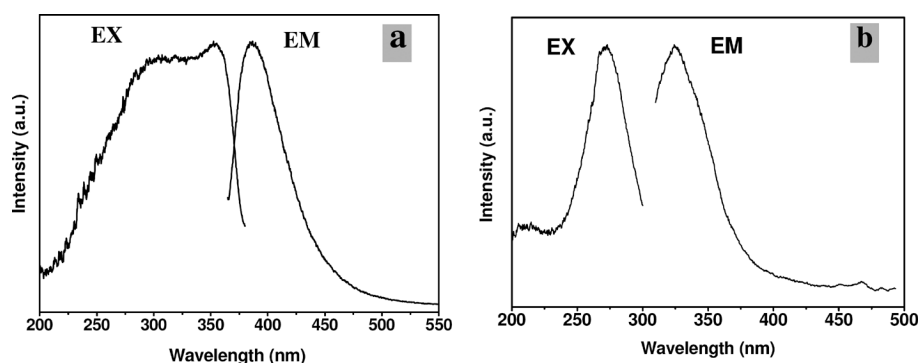


Figure 10. Excitation and emission spectra of compounds **1** (a) and **2** (b) at room temperature.

pounds possess good luminescent properties and may find potential applications in the fields of lighting, displays, or biomedicine.

## Acknowledgement

This work was supported by the *National Natural Science Foundation of China* (Grant No. 20771098) and the *Fund for Creative Research Groups* (Grant No. 20921002).

## References

- [1] a) O. M. Yaghi, M. O'Keeffe, N. W. Ockwig, H. K. Chae, M. Ed-  
daoudi, J. Kim, *Nature* **2003**, *423*, 705; b) S. R. Batten, R. Robson,  
*Angew. Chem. Int. Ed.* **1998**, *37*, 1460; c) L. Carlucci, G. Ciani,  
D. M. Proserpio, *Coord. Chem. Rev.* **2003**, *246*, 247; d) C. N. R.  
Rao, S. Natarajan, R. Vaidhyanathan, *Angew. Chem. Int. Ed.* **2004**,  
*43*, 1466.
- [2] a) S. A. Bourne, J. Lu, B. Moulton, M. J. Zaworotko, *Chem. Com-  
mun.* **2001**, 861; b) N. W. Ockwig, O. Delgado-Friederichs, M.  
O'Keeffe, O. M. Yaghi, *Acc. Chem. Res.* **2005**, *38*, 176; c) S. Kita-  
gawa, R. Kitaura, S. I. Noro, *Angew. Chem. Int. Ed.* **2004**, *43*,  
2334; d) O. R. Evans, W. Lin, *Acc. Chem. Res.* **2002**, *35*, 511; e) L.  
Carlucci, G. Ciani, D. M. Proserpio, *CrystEngComm* **2003**, *5*, 269.
- [3] a) S. R. Batten, K. S. Murray, *Coord. Chem. Rev.* **2003**, *246*, 103;  
b) M. L. Tong, X. M. Chen, S. R. Batten, *J. Am. Chem. Soc.* **2003**,  
*125*, 16170.
- [4] a) C.-D. Wu, W. Lin, *Angew. Chem. Int. Ed.* **2007**, *46*, 1075;  
b) B. F. Abrahams, S. R. Batten, M. J. Grannas, H. Hamit, B. F.  
Hoskins, R. Robson, *Angew. Chem. Int. Ed.* **1999**, *38*, 1475;  
c) S. R. Batten, B. F. Hoskins, R. Robson, *Angew. Chem. Int. Ed.*  
*Engl.* **1997**, *36*, 636.
- [5] a) P. Jensen, D. J. Price, S. R. Batten, B. Moubaraki, K. S. Murray,  
*Chem. Eur. J.* **2000**, *6*, 3186; b) J. M. Taylor, A. H. Mahmoud-  
khani, G. K. H. Shimizu, *Angew. Chem. Int. Ed.* **2007**, *46*, 795;  
c) M. Dan, C. N. R. Rao, *Angew. Chem. Int. Ed.* **2006**, *45*, 281.
- [6] a) S. Q. Liu, T. Kuroda-Sowa, H. Konaka, Y. Suenaga, M. Maek-  
awa, T. Mizutani, G. L. Ning, M. Munakata, *Inorg. Chem.* **2005**,  
*44*, 1031; b) X. M. Chen, G. F. Liu, *Chem. Eur. J.* **2002**, *8*, 4811.
- [7] J.-F. Ma, J. Yang, G.-L. Zheng, L. Li, J.-F. Liu, *Inorg. Chem.* **2003**,  
*42*, 7531.
- [8] G. M. Sheldrick, *SHELXS-97*, Program for X-ray Crystal Structure  
Solution, University of Göttingen, Göttingen, Germany, **1997**.
- [9] G. M. Sheldrick, *SHELXL-97*, Program for X-ray Crystal Structure  
Refinement, University of Göttingen, Göttingen, Germany, **1997**.

Received: August 12, 2010

Published Online: November 25, 2010